Supplementary information of

Chemical species of cesium and iodine in condensed vaporized microparticles produced by melting nuclear fuel components with concrete materials

Toshihiko Ohnuki[a,b,c] ,Jian Ye[a], Tomoaki Kato[b,d], Jiang Liu[d], Masahide Takano[d], Naofumi Kozai[e], and Satoshi Utsunomiya,[f]

[a] School of Resource Environment and Safety Engineering, University of South China, Zhengxiang District, Hengyang, Hunan, 421001, China

[b] Fukushima Reconstruction and Revitalization Unit, Institute of Innovative Research, Tokyo Institute of Technology, 2-12-1 Ookayama, Meguro-ku, Tokyo 152-8550, Japan

[c] The Institute of Human Culture Studies (IHCS), Otsuma Women's University, 12 Sanbancho, Chiyoda-ku. Tokyo 102-8357, Japan

[d] Collaborative Laboratories for Advanced Decommissioning Science (CLADS), Japan Atomic Energy Agency (JAEA), Tomioka, Fukushima, Japan

[e] Advanced Science Research Center, Japan Atomic Energy Agency (JAEA), Tokai, Ibaraki, 319-1195, Japan

[f]Department of Chemistry, Kyushu University, 744 Motooka, Nishi-ku, Fukuoka 819-0395, Japan

Table S1 1 Quantitative components in the three origin composites.

	Composite A	Composite B
	wt%	wt%
ZrO_2	87.8	40.5
CsI	2.3	4.1
SUS316	9.9	9.7
Concrete		45.7

SI for schematic diagram of the heating device and the experimental setup

Schematic diagram of the light-concentrated heating device [43].

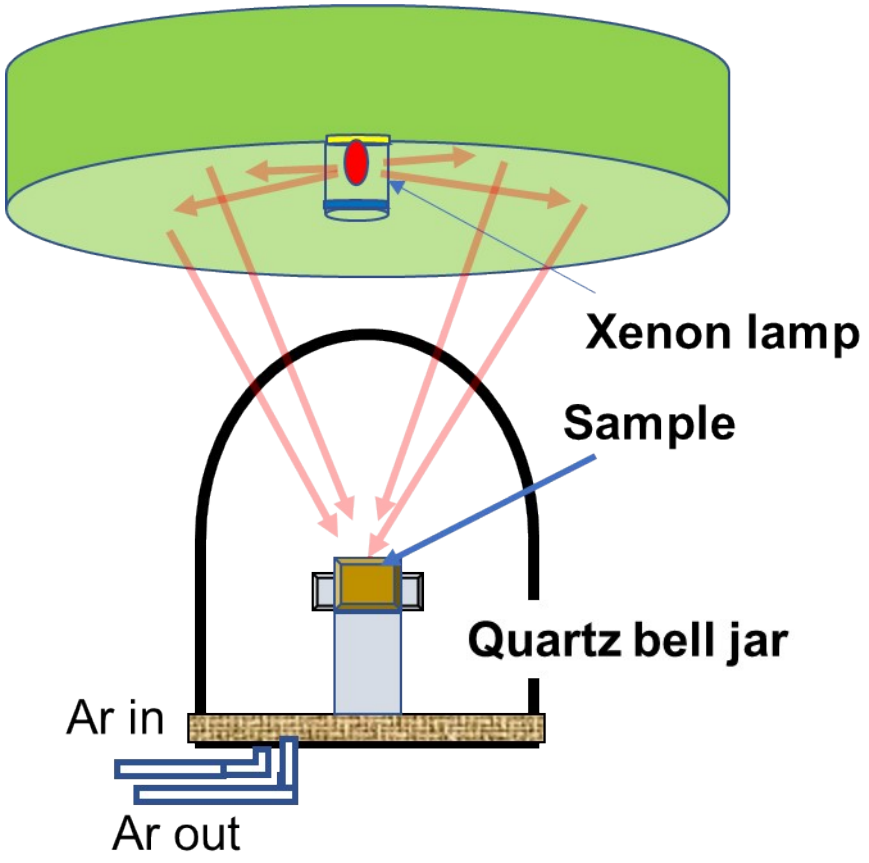

A light concentrated heating system (Crystal System Corporation, IRM-3000-X), in which

light from a xenon lamp, with maximum output of 3 kW, was concentrated onto the sample by a dome-type reflector. The lamp power was manually controlled based on the molten state by monitoring the sample during heating with a video camera. Because temperature measurement by a pyrometer was difficult due to the strong heat output from the lamp, the maximum temperature of the melt was estimated by phases observed in solidified samples to be > 2000 °C.

Schematic setup of the samples in the belle jar[43].

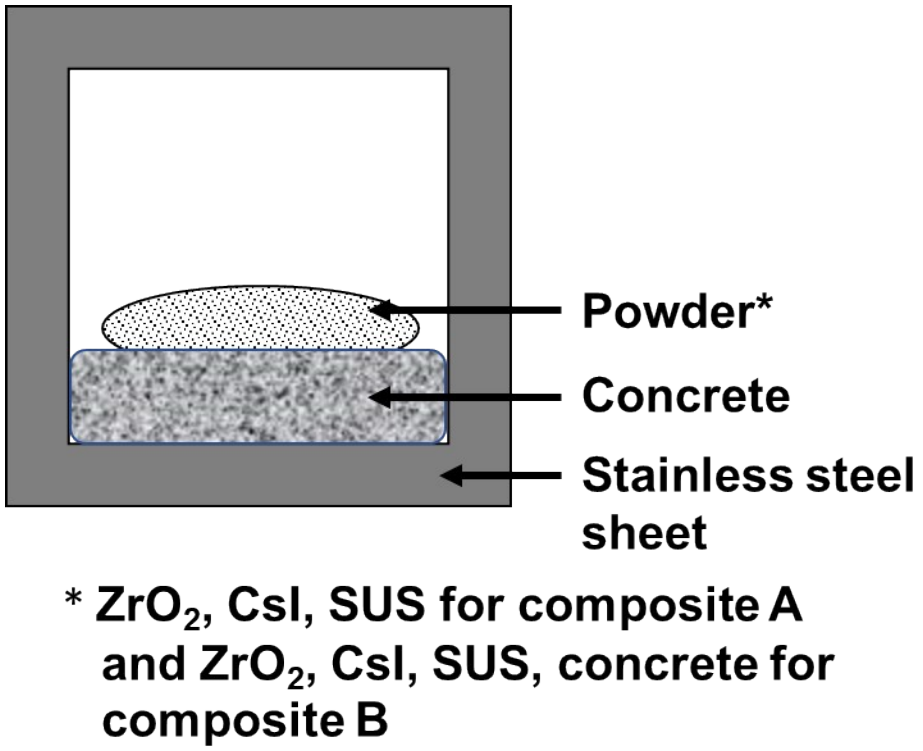

Table SI 2 Elemental compositions in at% of CVS A analyzed at points numbered 1 to 8 in Fig.

1a.

Element	O	Si	S	Cl	K	Cr	Fe	Ni	Zn	Zr	I	Cs	Total
Point													
1	41.1	2.7	7.0	0.3	0.5	2.0	2.0	6.3	0.1	0.4	15.3	22.5	100
2	67.0	6.3	3.5	0.4	0.5	4.1	6.4	8.6	0.2	0.5	0.5	2.0	100
3	26.3	1.5	3.7	0.3	0.4	1.5	1.9	5.4	0.1	0.4	23.9	34.5	100
4	63.6	5.7	4.2	0.4	0.5	5.4	6.1	11.9	0.1	0.3	0.4	1.4	100
5	61.3	5.4	4.7	0.3	0.5	3.1	3.8	9.7	0.2	0.3	4.1	6.5	100
6	26.3	1.3	1.8	0.1	0.1	1.0	0.8	3.6	0.4	0.2	26.2	38.1	100
7	56.7	5.2	4.8	0.4	0.6	3.3	4.6	8.0	0.4	0.2	6.0	9.7	100
8	64.5	6.5	4.0	0.3	0.9	5.0	8.8	8.0	0.2	0.4	0.4	1.2	100

Figure SI 1 Mapping images of Cs and I, and overlay mapping images of Cs and I in CVS A.

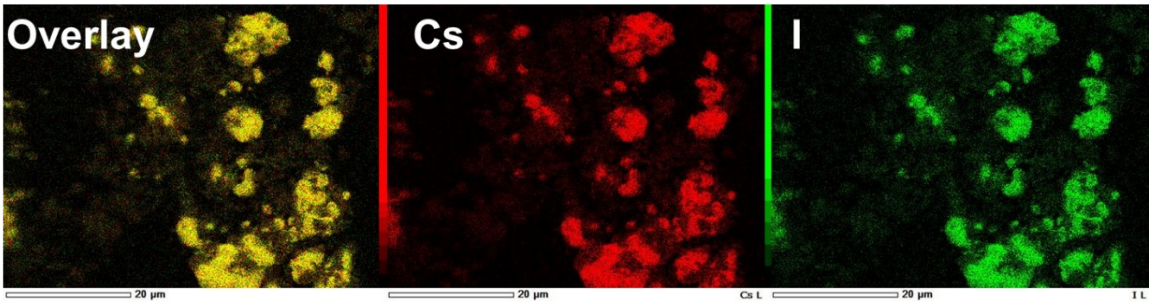

SI for Analysis of CVS A in different region from Fig. 1a.

The SEM image of CVS A in the different region from Fig. 1a (Figure SI 2) shows the presence of round particles less than 1 μm in diameter (numbered 1, 2, 3, and 4). In the EDX spectrum at position 1 (Figure SI 3), peaks of Si, Zr, S, Cl, K, I, Cs, Cr Fe, and Ni were distinguished. This result indicates that ~1 μm particles contained Si, Zr, S, Cl, K, I, Cs, Cr Fe, and Ni. The elemental components at positions 1 to 8 in Figure SI 2 are shown in Table SI 3. The contents of Si in the ~1 μm round particles were higher than those in particles 5 to 8, in which the particle diameters were larger than 1 μm in Fig. SI 2. The relationships between the at% of Si, and those of Cs and I are plotted as closed circles for Cs and closed rectangles for I in Fig. 1b. The at% of Cs and that of I were nearly constant regardless of the at% of Si. The contents of Cs were higher than those of I.

Figure SI 2. SEM image of CVS A. The position analyzed is different from that in Fig. 1a. Numbers show the positions analyzed by EDX.

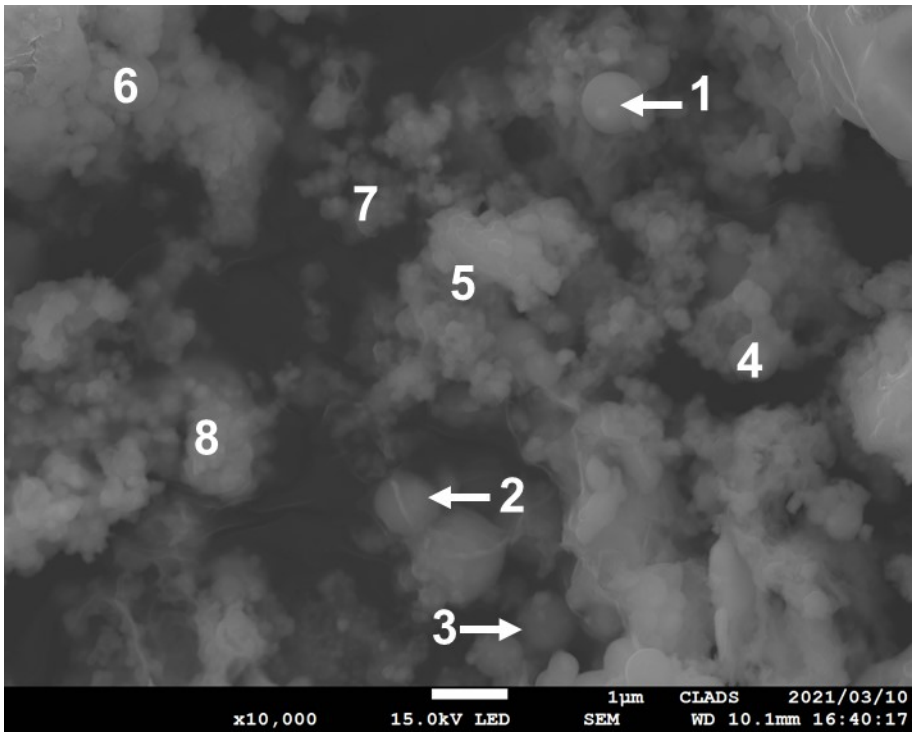

Table SI 3 Elemental compositions in at% of CVS A analyzed at points numbered 1 to 8 in Figure SI 2.

Element	O	Si	S	Cl	K	Cr	Fe	Ni	Zn	Zr	I	Cs	Total
Point													
1	71.4	10.7	2.2	0.2	0.7	3.1	5.9	3.7	0.1	0.2	0.4	1.3	100
2	69.9	14.0	1.3	0.1	0.7	1.9	7.5	2.2	0.1	0.3	0.1	1.9	100
3	67.4	11.1	3.1	0.1	3.2	2.9	6.9	2.3	0.2	0.2	0.6	2.1	100
4	67.6	6.9	4.5	0.2	0.6	3.3	6.4	7.4	0.4	0.3	0.5	1.8	100
5	65.3	4.0	5.4	0.4	0.5	3.5	3.0	14.7	0.2	0.3	1.0	1.7	100
6	55.7	7.8	4.4	0.6	0.8	4.6	6.6	12.7	0.2	0.4	1.8	4.4	100
7	66.2	2.8	5.5	0.3	0.3	5.0	4.1	13.2	0.1	0.5	0.4	1.5	100
8	60.4	6.3	3.3	0.3	0.6	7.0	8.1	11.2	0.2	0.2	0.6	1.7	100

Figure SI 3 EDX spectrum at position 1 in Figure SI 2.

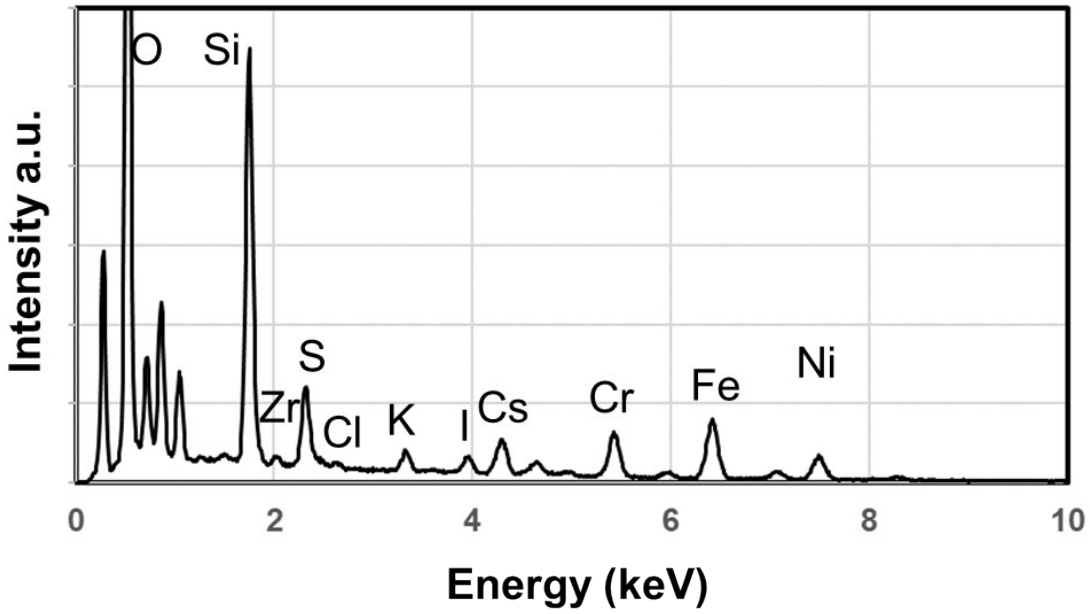

SI for Analyses for CVS B.

SEM photographs of CVS B (Figure SI 4) shows that particles less than ~5 μm and larger than ~10 μm in diameter were involved. Similar particles were present in different region (Figure SI 5). Element compositions in at% of the particles of 1, 2, and 5 in Fig. SI 4 (Table SI 4) and those of 2 and 4 in Fig. SI 5 (Table SI 5) indicate that Cs and I contents were high 30-49 at% for Cs and 20-30 at% for I, respectively, and Si contents were 2-3 at%. On the other hand, the at% of Si in the particles less than 3 μm in diameter shown by 3 and 4 in Fig. SI 4 and by 1, 3, and 5 in Fig. SI 5 were 3 to 5 times as much as those in the large particles 1, 2, and 5 in Fig. SI 4 and 2 and 6 in Fig. SI 5. Note that in larger particles than ~10 μm, large amounts of Cs and I were detected. Element mapping images of Cs, I, and Si and the overlay mapping image (Figure SI 6) show that two types of the particles were present in CVS B. First one is green color particles in the overlay mapping image containing mainly Si. Second one is pink color particles containing I and Si. No red color particle was distinguished in the overlay image, indicating that most of Cs in CVS B were present with I.

From the relationship of at% of Cs or I and at% of Si (Figure SI 7), when the Si content was low of ~2 at%, the Cs was high of 30~45 at%. When the content of Si was ~5 at% or higher, the Cs was less than ~2 at% as denoted by arrow, which is almost unchanged. Regarding I, manner of I resembled that of Cs. These results are likely to be presence of I with Cs, which is consistent with the overlay mapping image in Fig. SI 6.

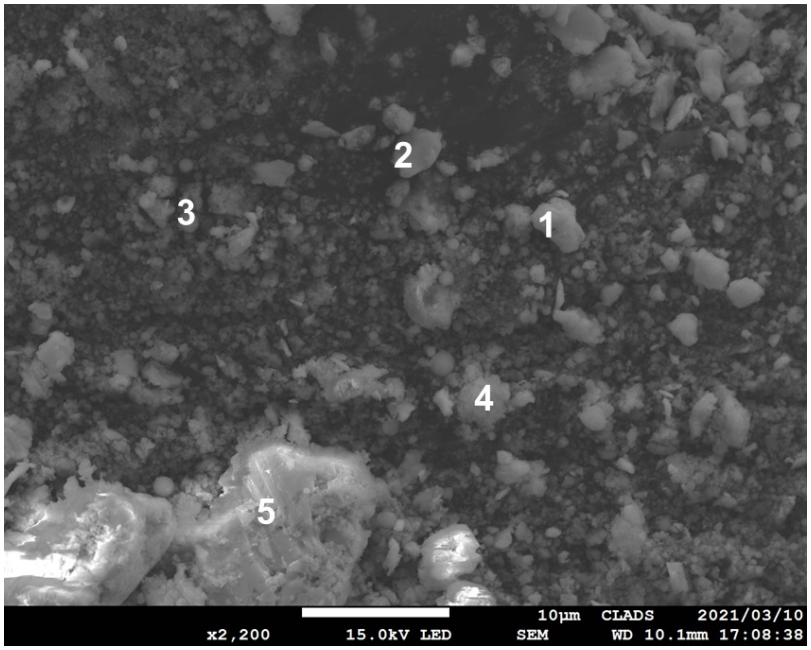

Figure SI 4 SEM photographs of CVS B. Numbers show the positions analyzed by EDX.

Table SI 4 Elemental compositions in at% of CVS B analyzed at points numbered 1 to 5 in Fig. 3.

Element	O	Si	S	Cl	K	Cr	Fe	Ni	Zn	Zr	I	Cs	Total
Point													
1	18.7	2.0	0.9	0.0	0.6	0.4	0.2	0.7	1.5	0.3	30.5	44.1	100
2	15.8	2.0	0.9	0.1	0.9	0.2	0.3	0.5	0.9	0.3	31.8	46.3	100
3	70.8	5.5	3.9	0.5	2.2	3.7	1.5	3.5	3.0	2.1	0.8	2.4	100
4	63.1	8.4	2.4	0.2	8.6	1.7	1.6	2.2	2.3	1.0	5.9	2.4	100
5	34.5	3.1	1.9	0.3	1.1	1.0	0.8	1.4	1.5	0.8	22.0	31.7	100

Figure SI 5 SEM photographs of CVS B. The region analyzed is different from Fig. 3. Numbers show the positions analyzed by EDX.

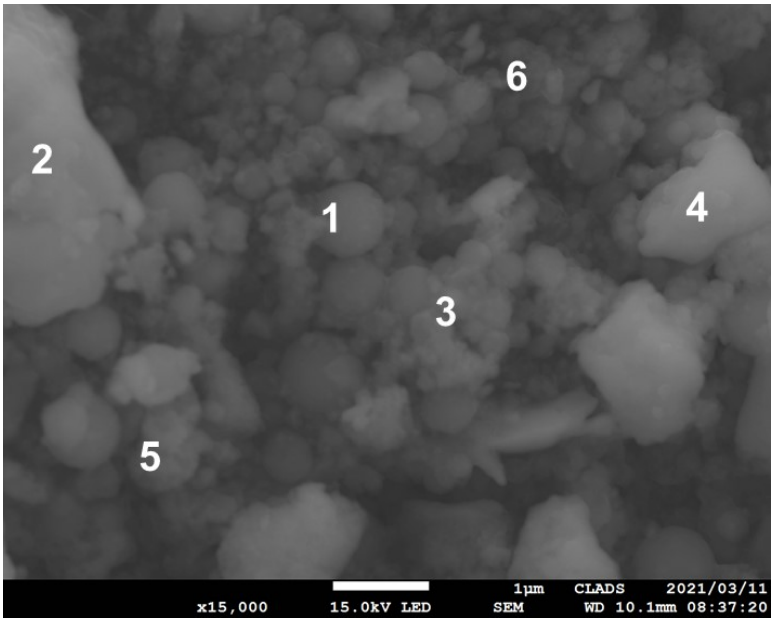

Table SI 5 Elemental compositions in at% of CVS B analyzed at points numbered 1 to 6 in Figure SI 5.

Element	O	Si	S	Cl	K	Cr	Fe	Ni	Zn	Zr	I	Cs	Total
Point													
1	75.1	15.5	0.5	0.1	0.8	1.6	2.3	1.0	0.5	0.5	0.5	1.5	100
2	14.3	2.0	0.6	0.0	0.5	0.0	0.3	0.4	0.2	0.3	32.6	49.0	100
3	73.1	11.3	1.6	0.2	1.4	1.9	1.9	2.0	1.6	0.9	1.3	2.6	100
4	40.4	5.5	1.5	0.1	0.9	0.8	0.6	0.8	0.8	0.7	19.0	28.8	100
5	61.9	6.9	3.1	0.3	2.7	2.7	1.3	3.9	9.6	3.4	1.6	2.6	100
6	75.3	3.9	4.1	0.3	2.0	1.8	0.8	2.8	4.5	1.3	1.3	1.9	100

Figure SI 6. Elemental mapping images of Cs, I, and Si and the overlay mapping image of those elements in CVS B.

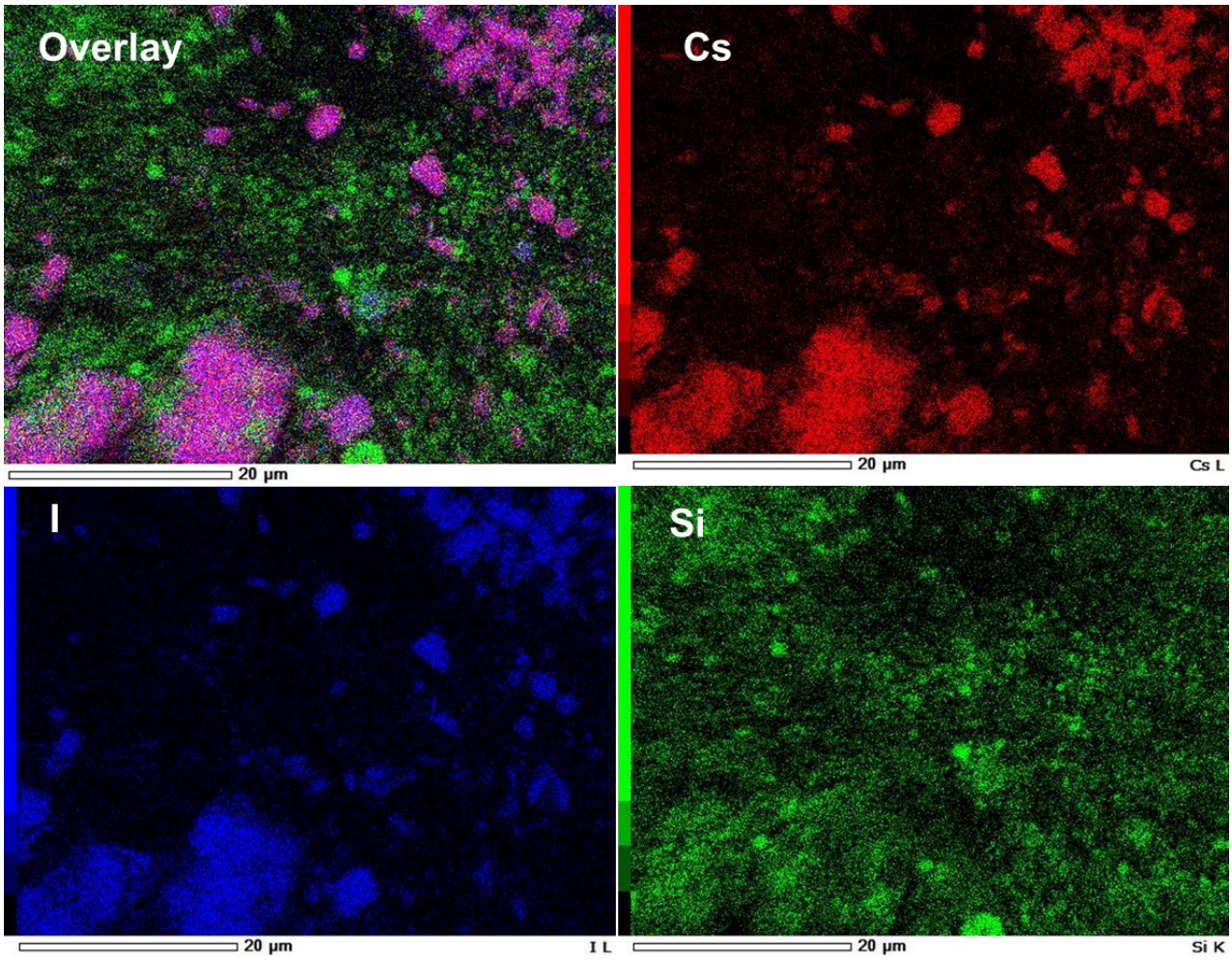

Figure SI 7. Relationship between Si contents and those between Cs and I of CVS B. When the Si content was low of ~2 at%, Cs was high of 30~45 at%. When the content of Si was ~5 at% or higher, Cs was less than ~2 at% as denoted by arrow, which is almost unchanged.

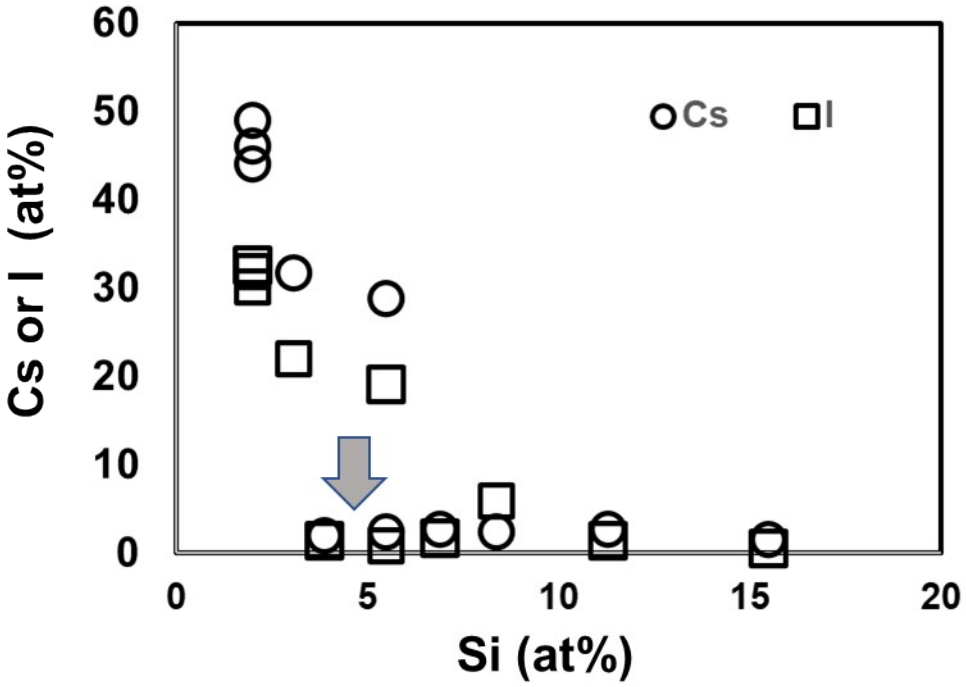

Figure SI 8. Difference between standard spectrum and CVS ones. (a) I L_{III} edge spectra and (b) Cs L_{III} edge spectra.

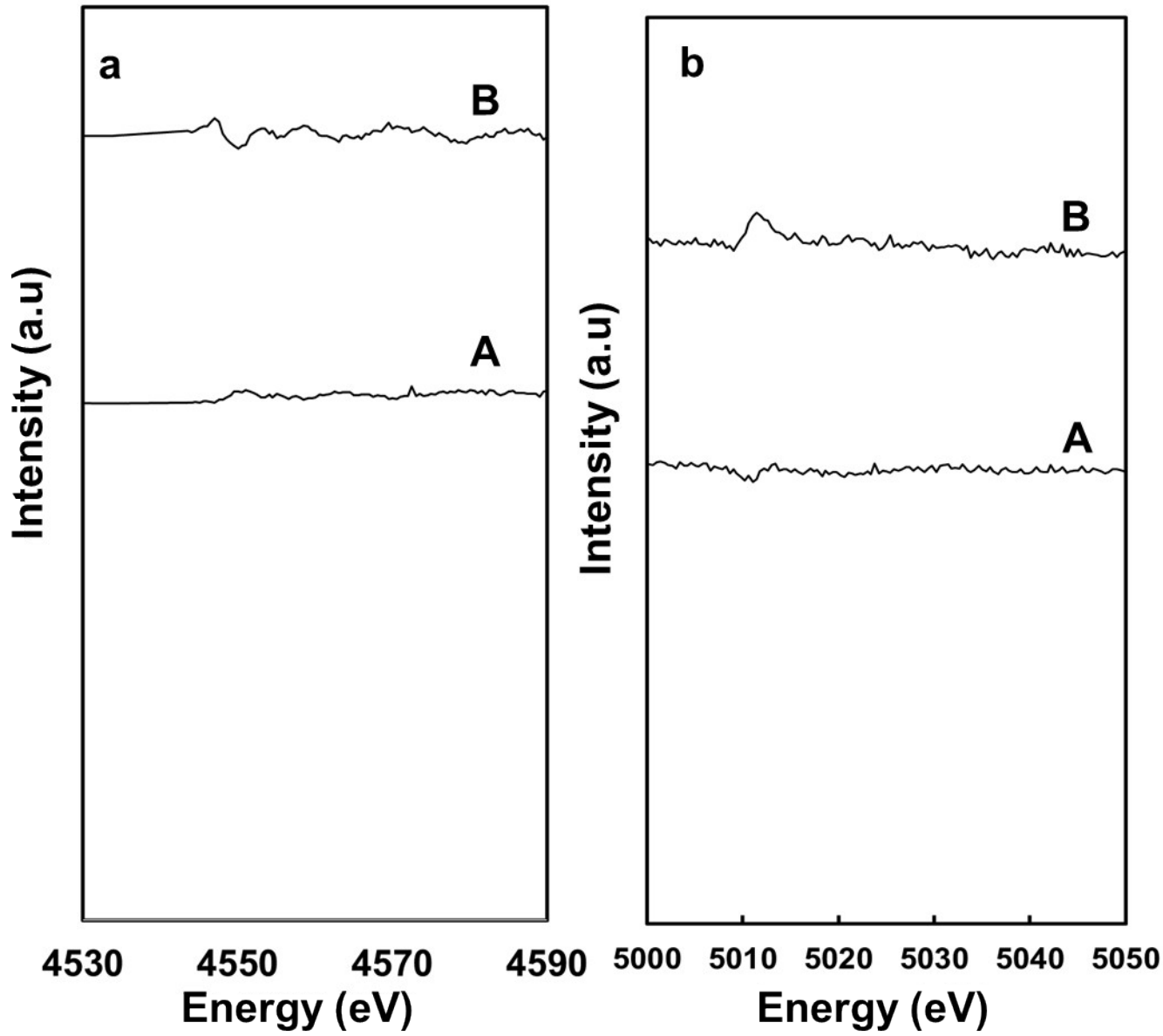

Table SI 6 Elemental compositions in at% of CVS A treated with deionized water analyzed at points numbered 1 to 6 in Fig. 4.

Element	O	Si	S	Cl	K	Cr	Fe	Ni	Zn	Zr	I	Cs	Total
Point													
1	69.8	6.7	3.4	0.1	0.4	4.5	6.4	6.8	0.2	1.0	0.0	0.7	100
2	86.4	3.6	2.0	0.2	0.3	1.0	1.3	3.3	1.4	0.3	0.0	0.3	100
3	73.1	5.0	2.5	0.1	0.3	3.8	4.9	9.1	0.3	0.6	0.0	0.4	100
4	71.2	3.8	3.8	0.1	0.2	4.1	4.6	10.8	0.2	0.7	0.1	0.3	100
5	70.2	4.2	4.8	0.1	0.2	4.0	3.7	10.9	0.2	1.0	0.0	0.4	100
6	65.9	8.2	2.5	0.1	0.4	5.6	11.2	4.9	0.2	0.3	0.0	0.8	100

Figure SI 9 Overlay mapping image of Cs, Si, and Fe of the yellow rectangular area in Fig. 4, and individual element mapping images of the water treated CVS A.

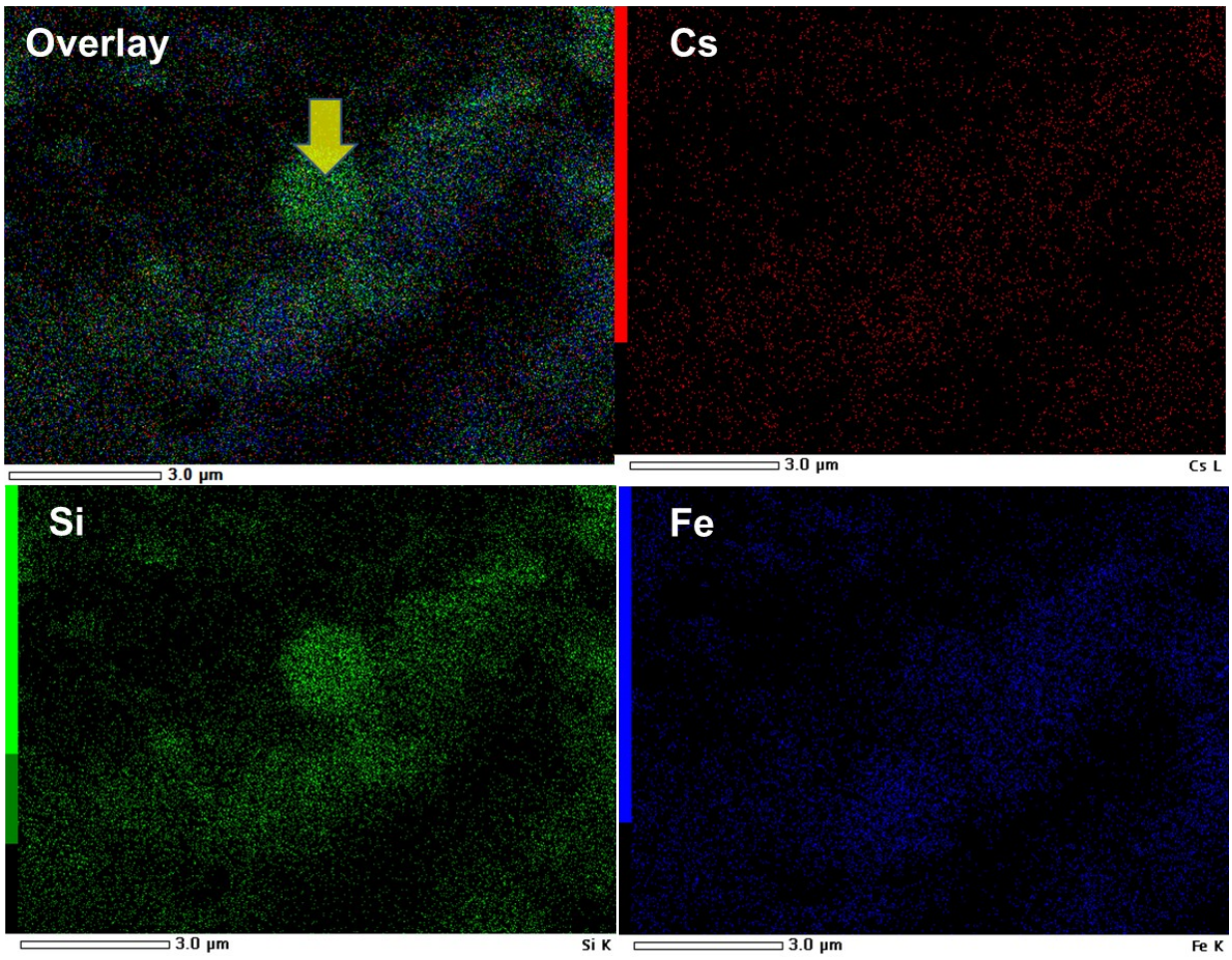

Figure SI 10 SEM photograph of CVS B after water treatment. Red circle shows presence of nano sized particles.

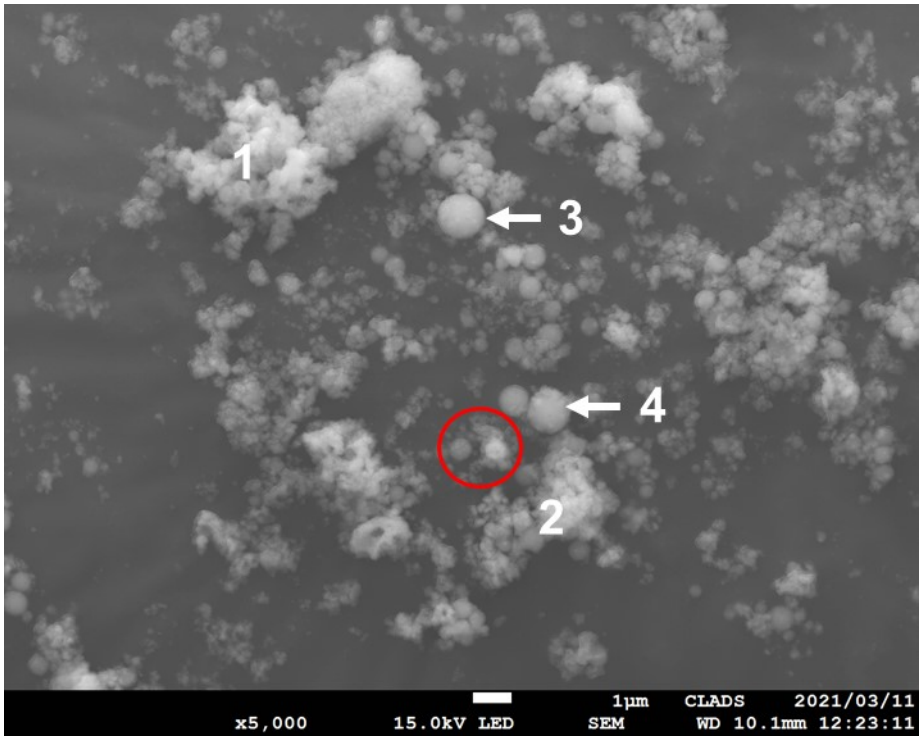

Table SI 7 Elemental compositions in at% of CVS B treated with deionized water analyzed at points numbered 1 to 4 in Figure SI 10.

Element	O	Si	S	Cl	K	Cr	Fe	Ni	Zn	Zr	I	Cs	Total
Point													
1	74.7	3.8	4.0	0.1	1.5	3.2	1.0	3.2	3.1	2.1	0.1	3.1	100
2	71.5	3.8	3.8	0.2	1.7	2.0	1.1	3.9	5.8	3.2	0.1	2.9	100
3	74.2	14.6	0.5	0.0	2.7	2.1	2.4	1.2	0.4	0.6	0.0	1.3	100
4	75.6	13.3	0.7	0.0	2.1	1.9	2.3	1.3	0.6	0.6	0.0	1.7	100

Figure SI 11 SEM photograph of CVS B after treated with deionized water. The region analyzed was different from Figure SI 10.

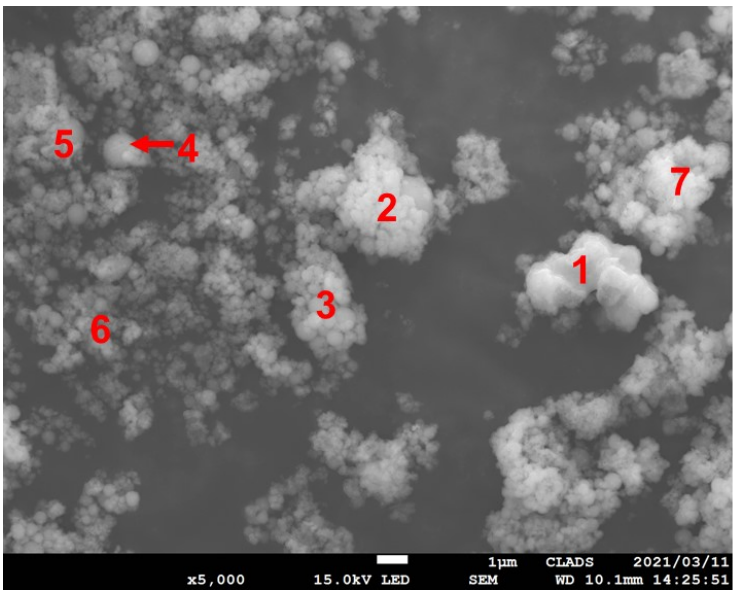

Table SI 8 Elemental compositions in at% of the deionized water treated CVS B analyzed at points numbered 1 to 7 in Fig. SI 11.

Element	O	Si	S	Cl	K	Cr	Fe	Ni	Zn	Zr	I	Cs	Total
Point													
1	72.3	4.8	7.1	0.2	2.8	1.4	0.9	3.1	4.9	1.3	0.2	0.9	100
2	72.4	13.6	1.3	0.1	2.0	2.4	2.0	2.0	1.6	0.9	0.0	1.8	100
3	73.2	14.2	1.0	0.1	1.1	2.3	2.5	1.9	1.5	0.8	0.0	1.4	100
4	79.7	7.6	1.3	0.1	1.2	1.6	1.4	1.6	3.0	1.4	0.0	1.2	100
5	71.7	6.9	3.1	0.1	1.4	2.8	1.2	3.8	5.7	2.0	0.0	1.2	100
6	74.4	10.5	1.8	0.1	1.2	2.5	2.3	2.3	2.7	1.1	0.0	1.1	100
7	83.5	3.1	2.9	0.2	1.2	0.5	0.4	2.0	4.6	1.1	0.0	0.6	100

Figure SI 12 Relationships between contents of Si and those of Cs and I (a) and between Cs and Fe, Cr, Ni, and Zn (b) of the water-treated CVS B.